Sciencia Acta Xaveriana
An International Science Journal
ISSN. 0976-1152

Volume 7
No. 1
pp. 29-36
March 2016

XPRD and electrical measurements of NH_4SbF_4 Single Crystals

R. Mary Jenila*

* Physics Research Centre, St. Xavier's College (Autonomous), Palayamkottai, Tirunelveli–627 002, Tamil Nadu, India

Abstract

Ammonium Tetra Fluoro Antimonate (ATFA) with chemical formula NH_4SbF_4 is grown by slow evaporation technique from aqueous solution. X –ray Powder diffraction analysis were carried out for the position ranging from 0 to 80° for defining the d- spacing and to assign the hkl parameters. Electrical measurements are carried out along the a - axis of the grown crystal at various temperatures by the conventional parallel plate capacitor method. The present study shows the dielectric behaviour and the conductivity measurements of ATFA crystals. Dielectric constant and dielectric loss have been measured as a function of frequency for various ranges of temperatures. AC electrical conductivity is also studied for the grown crystal at various temperature range and the activation energies are reported in detail.

Keywords: ATFA, XPRD, SbF_3, NH_4F, dielectric constant, AC conductivity

(Received : 29th December 2015 ; Accepted : 20th February 2016)

1. Introduction

The study of physicochemical properties of inorganic fluorides is gaining interest because of the extensive possibilities for their applications in optical instruments and laser technology [1]. There have been extensive investigations on the fluoro antimonates single crystals due to their unique properties such as large band gap and has many optical advantages [2-3]. Ammonium fluoro antimonates are of interest which leads to higher electrical conductivity and behaves as good ionic conductors [4-5]. Among the high ionic conductivity compounds are some antimony (III) fluorides with univalent cations [6-9]. The crystal structure of ATFA was reported by Ovchinnikov et al as monoclinic with a cenro symmetric phase group P21/a [10]. The optical,

thermal and hardness properties of ATFA are reported earlier [11]. In this paper, the powder x-ray peak assignments, dielectric and conductivity measurements of ATFA are discussed in detail.

2. Experimental Details

Appropriate stoichiometric ratios of Ammonium fluoride (NH_4F) and Antimony tri fluoride (SbF_3) are mixed together to prepare the solutions of ATFA. The crystals are grown by slow evaporation technique at a constant temperature of 30°C. Crystals obtained by spontaneous nucleation are used as seeds to grow bulk crystals. Clear transparent single crystals with good morphology with size 10 x 8 x 7 mm^3 are obtained in a period of 30 days. The harvested crystal is shown in Figure 1.

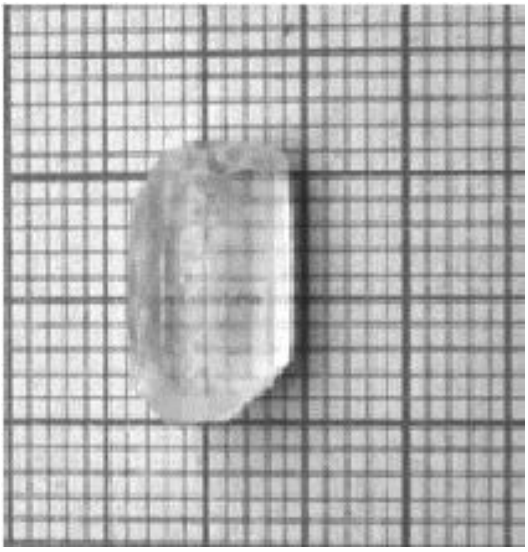

Fig.1. As grown ATFA single crystals

3. Characterisation

The grown crystals is subjected to powder X-ray analysis using a PANalytical powder X-ray diffractometer using nickel filtered cu k_α radiations with λ= 1.5405Å. The sample is scanned over the required range of 2θ varies from 10°to 80°. The crystalline phase structure of the ATFA crystals is identified from the crystallographic parameters such as 2θ, d-spacing, relative intensity and hkl parameters, the crystals with high transparency and large surface defect free without any cracks or scratch on the surface. The opposite faces are polished and coated with good quality of graphite to obtain better conductive surface layer. The capacitance (C_{crys}) and dielectric loss factor (tan δ) were observed using the conventional parallel plate capacitor method for different frequencies using an LCR Hi tester –MT 4090 LCR meter at various temperatures ranging from 313K to 423K to remove water molecules if present in the sample.

The observations are made when cooling the sample. The temperature is controlled by an accuracy of +1°C. The dimensions of the sample are measured using a travelling microscope with L.C =0.001cm. The dielectric constant of the ATFA single crystals are calculated using the relation

$$\varepsilon_r = C_c / C_a$$

Where C_c is the capacitance of the crystal and C_a is the capacitance of air. As the crystal area is smaller than the plate area of the cell, parallel capacitance of the portion of the cell not fitted with the crystal was taken into account and consequently the above equation becomes

$$\varepsilon_r = \left[\frac{C\,crys - Cair\left(1 - \frac{A\,cry}{A\,air}\right)}{C\,air}\right]\left(\frac{A\,air}{A\,cry}\right)$$

Where A_{cry} is the area of the crystals touching the electrode. Estimated standard deviation is determined by repeating the experiment several times and the overall inaccuracy involved in this measurement is found to be within +4%.

The *AC* conductivity (σ_{ac}) is calculated using the relation

$$\sigma_{ac} = \varepsilon_r \varepsilon_o \omega \tan \delta$$

Where ε_o is the permittivity of free space (8.85 x 10^{-12} farad/m) and $\omega = 2\pi f$ is the angular frequency. A plot drawn between ln σ_{ac} and 1000 /T are found to be very linear. So, the conductivity values can be fitted to the relation

$$\sigma_{ac} = \sigma_o \exp\left(\frac{-Eac}{KT}\right)$$

Where E_{ac} is the activation energy. The activation energies are estimated using the slope of the above line plots

$$E = -[(\text{slope})\,K] \times 1000$$

Where K is the Boltzmann constant, T is the absolute temperature and σ_o is the parameter depending upon the material.

4. Results and discussion

4.1 Powder X-ray diffraction

The X-ray powder diffraction patterns of ATFA are shown in Fig.2. The well defined peaks at specific 2θ values show the high crystalline nature of the grown crystals. The reflection peaks of Powder XRD patterns were indexed using UNITCELL software package. The highest

intensity peak is seen along the (0 2 1) plane. The d- spacing and the hkl indexed values are tabulated in table 1.

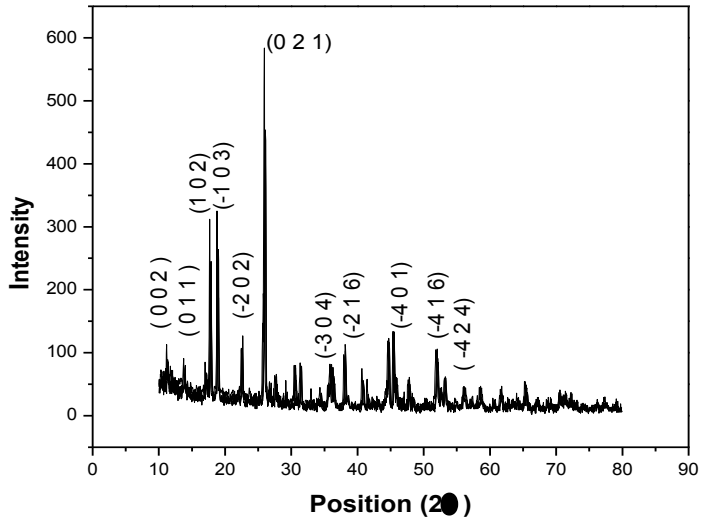

Fig.1. Powder XRD spectra of ATFA single crystals

Table 1. Powder XRD data for ATFA single crystals

S.No	2θ (degrees)	d-Values (Å)	hkl	Relative Intensity (%)
1	17.8400	4.96790	2 0 1	50.17
2	18.9582	4.67734	- 2 1 1	41.99
3	22.6115	3.92920	- 2 0 2	15.90
4	26.0518	3.41760	0 2 1	100.00
5	31.4846	2.83918	- 3 2 1	14.36
6	35.9918	2.49329	- 4 0 3	16.95
7	38.1361	2.35788	-5 2 0	24.83
8	44.7203	2.02483	- 6 2 2	23.19
9	45.5258	1.99086	- 4 3 1	24.64
10	52.0166	1.75666	- 6 3 1	21.07

4.2 Dielectric measurements

The variation of dielectric constant (ε_r) and dielectric loss (tanδ) with increase in temperature for frequencies ranging from 1 KHZ to 1 MHZ is shown in Fig.3. The dielectric constant is low for high frequencies and high for low frequencies. The dielectric constant of a material is generally composed of four types of contributions, viz ionic, electronic, orientation and space charge polarization. At low frequencies, all polarizations are operative and hence εr is high. As the frequency increases, one polarization after another frozen out. The first to stop contribution of ε_r is the orientational component, then the ionic and electronic polarization lastly [10-11]. The large value of ε_r at low frequency is due to the presence of space charge polarizations which depends on the purity and perfection of the crystals [12]. Fig.4 shows the variation of dielectric loss with varying frequency. The dielectric loss decreases with increase in frequency and is independent beyond 10KHZ. This may be due to the more concentration of defects formed in the crystal lattice [13].

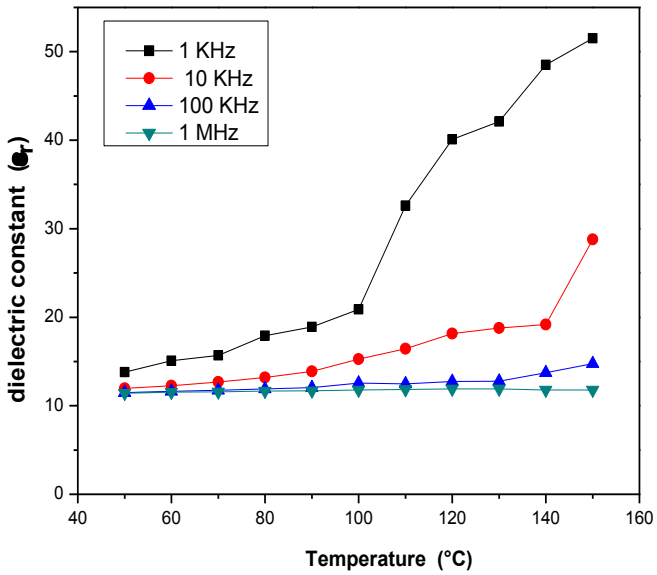

Fig.3. Variation of dielectric constant (ε_r) vs temperature (T) for ATFA crystal

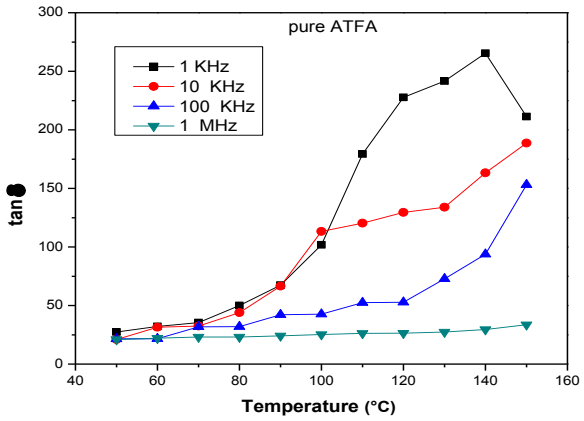

Fig.4. Variations of dielectric loss (tanδ) with temperature (T) for pure ATFA crystal

4.3 AC conductivity measurements

The *AC* conductivity measurements are carried out for the grown ATFA crystals for different range of frequencies at temperatures varying from 50 to 150°C are shown in Fig.5. The ac conductivity of ATFA increases as the temperature increases. Conduction in ionic crystals is due to the protonic movement of ions which enhances the increase in conductivity at low frequency. The conductivity at low frequencies is mainly due to the intrinsic conduction which creates more thermally agitated vacancies and mobility.

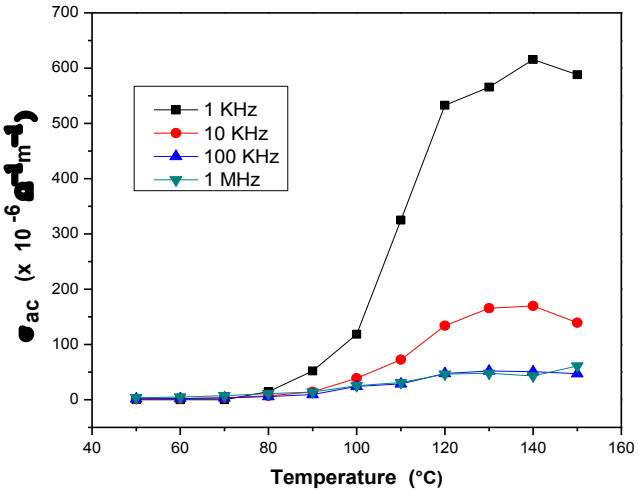

Fig.5 . Variation of *ac* conductivity (σ_{ac}) versus temperature (T) for ATFA Crystal

The variation of ln σ_{ac} with 1000/T for various frequencies are shown in Fig.6. The slope of the graph drawn between ln σ_{ac} with 1000/T gives the ac activation energies for various frequencies. The calculated activation energies for various frequencies are listed in Table 2. The low ac activation energy at high frequency region suggests that the more fluorine vacancies created are responsible for the conduction in the grown ATFA crystals.

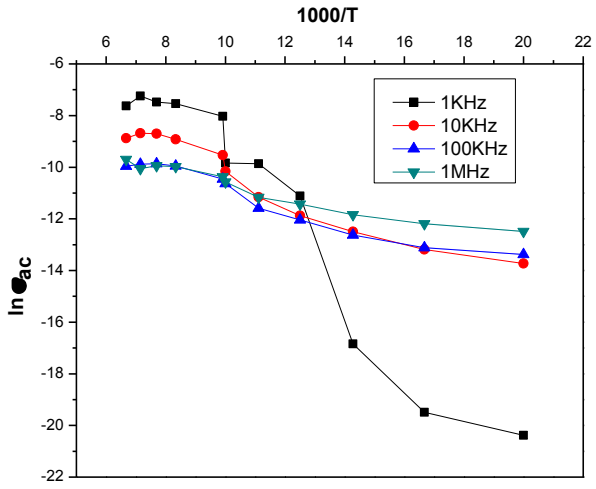

Fig.6. Variation of ln σ_{ac} with 1000 /T for ATFA single crystals

Table 3.4 *AC* activation energies for the ATFA crystals

Frequency	AC activation energy
10^4 Hz	0.03758
10^5 Hz	0.02468
10^6 Hz	0.01952

5. Conclusion

Single crystals of ATFA is grown by slow evaporation technique. The d-spacing, hkl parameters and relative intensity are calculated using powder XRD analysis. Electrical behaviour of ATFA is studied by measuring the dielectric and *AC* conductivity measurements. The

dielectric constant and dielectric loss posses low value in the higher frequency region due to the presence of space charge polarization. *AC* conductivity increases with increase in temperature due to the mobility of ions at higher temperature region. Low *ac* activation energies are observed with increase in frequency due to the presence of higher defect concentration in the ATFA single crystals.

Reference

1. Benet Charles. J., Gnanam .F.D., Materials Chem. and phy., 38 (1994)337
2. Mori.Y., Yap. Y.K., Kamimura.T., Yoshimura. M., Sasaki.T., Opt. Materials, 19 (2002)1
3. Zhengdong Li, Kechen Wu, Genbo Su, Youing He, Opt. Mater., 20 (2002) 295
4. Kavun.V.Ya., Uvarov.N.F., Slobdyuk. A.B., Brovkina. O.V., Zemnukhova. L.A., Sergienko.V.I., J. Electro Chem., 41 (2005) 560
5. Ovchinnikov.V.E., Udovenko.A.A., Solovena.L.P., Volkova.L.M., and Davidovich. R.L., Koord. Khim., 8 (1985) 697.
6. Borzenkhova.M.P., Kalinchenko. F.V., Novoselova.A.V., Ivanov.A.K., and Sorokin. N.I., Neorg.Khim., 29 (1984) 703
7. Yamada. K., Ohnuki. H., Okuda. T., Chem. Lett., 7 (1999) 627
8. Kotru. P.N., Ashok. K. Razdan., Wanklyn. B.M., J. Mater. Sci., 24 (1989) 793
9. Kavun. V.Ya., Sergienko. V.I., Sorokin. N.I., Zemnukohova. L.A., Kaidalova. T. A., and Mekulov. E.B., J. Struct. Chem., 42 (2001) 570
10. Shanmugham .M., Gnanam.F.D., Ramasamy .P., Ind. J. Pure and Appl. Phy., 20(1982) 579
11. Mary Jenila.R., Vetha photheher. I., Vimalan. M., Rajasekaran. T.R., J. Mater. Sci., 26(2015) 9
12. Narasimha.B., Choudhary.R.P., and Rao. K.V., J. Mater. Sci., 23 (1988) 1416
13. Goma.S., Padma.C.M., Mahadevan.C.K., Mater. Lett., 160 (2006) 370.